Low-power all-optical switching in active semiconductor chirped periodic structures

Drew N. Maywar and Govind P. Agrawal

The Institute of Optics and
Rochester Theory Center for Optical Sciences and Engineering
University of Rochester, Rochester, NY 14627, USA

maywar@optics.rochester.edu

Abstract: We investigate the effects of spatial chirp of the built-in grating on the spectral range and switching power of all-optical switching in active semiconductor periodic structures. We show that a total linear variation in the grating period of as little as 0.24% nearly triples the spectral range of low-power switching. Moreover, the upward-switching power at the onset of bistability is lowered by two orders of magnitude, to a value below 10 nW for typical device-parameter values. These improvements occur for optical signals tuned to the long-wavelength side of the stop band and propagating in the direction of increasing grating period. We also predict the existence of multiple bistable hystereses in devices with large amounts of spatial chirp.

OCIS codes: (250.5980) Semiconductor optical amplifiers; (999.9999) Optical switching; (230.1150) All-optical devices; (060.4510) Optical communications; (190.4360) Nonlinear optics, devices; (050.2770) Gratings.

References

1. G. P. Agrawal, Ed., *Semiconductor Lasers: Past, Present, and Future*, (AIP Press, New York, 1995).
2. M. J. Adams and R. J. Wyatt, "Optical Bistability in distributed feedback semiconductor laser amplifiers," IEE Proc., Pt. J **134**, 35–40 (1987).
3. K. Otsuka and S. Kobayashi, "Optical Bistability and Nonlinear Resonance in a Resonant-Type Semiconductor Laser Amplifier," Electron. Lett. **19**, 262–263 (1983).
4. R. P. Webb, "Error-rate measurements on an all-optically regenerated signal," Opt. Quantum Electron. **19**, S57–S60 (1987).
5. N. Ogasawara and R. Ito, "Static and Dynamic Properties of Nonlinear Semiconductor Lasers Amplifiers," Jpn. J. Appl. Phys. **25**, 739–742 (1986).
6. W. F. Sharfin and M. Dagenais, "High Contrast, 1.3 μm optical AND gate with gain," Appl. Phys. Lett. **48**, 1510–1512 (1986).
7. Z. Pan and M. Dagenais "Bistable Diode Laser Amplifiers as Narrow Bandwidth High-Gain Filter for Use in Wavelength Division Demultiplexing," IEEE Photon. Tech. Lett. **4**, 1054–1057 (1992).
8. H. J. Westlake, M. J. Adams, and M. J. O'Mahony, "Measurement of Optical Bistability in an InGaAsP Laser Amplifier at 1.5 μm," Electron. Lett. **21**, 992–993 (1985).
9. W. F. Sharfin and M. Dagenais, "Femtojoule optical switching in nonlinear semiconductor laser amplifiers," Appl. Phys. Lett. **48**, 321–322 (1986).
10. K. Tada and Y. Nakano, "Semiconductor Photonic Integrated Devices," Electron. Commun. Japan **77**, 238–249 (1994).
11. M. J. Adams, H. J. Westlake, and M. J. O'Mahony, "Optical Bistability in 1.55 μm Semiconductor Laser Amplifiers," in *Optical Bistability III*, H. M. Gibbs, P. Mandel, N. Peyghambarian, S. D. Smith, Ed. (Springer, Berlin, 1986).
12. G. Assanto and R. Zanoni, "Almost-Periodic Nonlinear Distributed Feedback Gratings," Opt. Acta **34**, 89–101 (1987).
13. G. Assanto, R. Zanoni, and G. I. Stegeman, "Effects of Taper in Nonlinear Distributed Feedback Gratings," J. Mod. Opt. **35**, 871–883 (1988).
14. S. Radic, N. George, and G. P. Agrawal, "Theory of low-threshold optical switching in nonlinear phase-shifted periodic structures," J. Opt. Soc. Am. B **12**, 671–680 (1995).
15. J. Liu, C. Liao, S. Liu, and W. Xu, "The dynamics of direction-dependent switching in nonlinear chirped gratings," Opt. Commun. **130**, 295–301 (1996).

#6998 - $15.00 US Received October 01, 1998; Revised October 19, 1998

16. S. Radic, N. George, and G. P. Agrawal, "Generalized distributed feedback design: amplification, filtering and switching," SPIE Proc. **2399**, 37–48 (1995).
17. D. N. Maywar and G. P. Agrawal, "Transfer-Matrix Analysis of Optical Bistability in DFB Semiconductor Laser Amplifiers with Nonuniform Gratings," IEEE J. Quantum Electron. **33**, 2029–2037 (1997).
18. M. Yamada and K. Sakuda, "Adjustable gain and bandwidth light amplifiers in terms of distributed-feedback structures," J. Opt. Soc. Am. A **4**, 69–76 (1987).

1. Introduction

Active semiconductor periodic structures of the kind depicted in Fig. 1(a) are routinely used as the basis of distributed feedback (DFB) lasers [1]. Driven *below* lasing threshold, these devices exhibit resonances that provide strong amplification for signals tuned near the stop-band edges, as shown in Fig. 1(b). Optical signals incident on such a resonant-type semiconductor optical amplifier (SOA) can exhibit dispersive bistability [1], [2]. Indeed, bistable SOAs have been used to demonstrate optical switching [3], signal regeneration [4], power limiting [5], memory [5], optical logic [6], and wavelength-division demultiplexing [7].

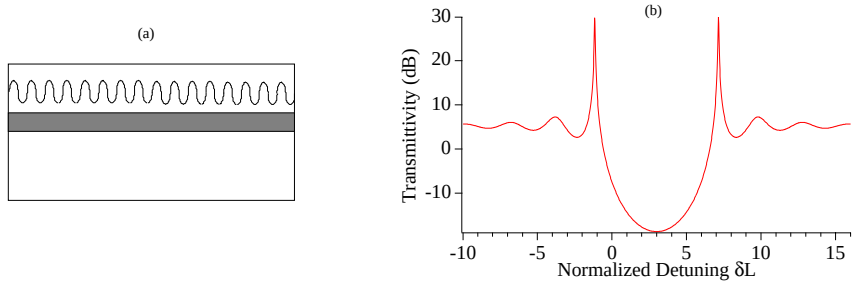

Figure 1. (a) Schematic of an active semiconductor periodic structure. The grating is typically fabricated outside of the active region (shaded grey). (b) Small-signal transmittivity spectrum for the device driven to provide 30-dB amplification at the resonance peaks. The detuning parameter δ is given by Eq. (4).

Bistable switching in resonant-type SOAs has been measured at *microwatt* power levels [8]. Such a low switching power is, in part, due to a strong nonlinearity, which arises from the dependence of the refractive index on the carrier density within the semiconductor amplifier [1]. The corresponding value of the effective n_2 ($\sim 10^{-9}$ cm^2/W) is seven orders of magnitude larger than measured for silica fibers. A low switching power allows bistable SOAs, which exhibit a switching speed $\sim$ 1 ns, to operate at femtojoule energies ($\sim$ 7000 photons) [9].

Optical switching in DFB SOAs is advantageous to fiber-optic communication systems because switching can occur at available power levels, typically 1 mW or less. In addition, SOAs can be fabricated to operate at any wavelength used in lightwave systems [1]. Since SOAs are compact (< 500 μm^3 active volume), many devices can be integrated into a monolithic photonic circuit and combined with lasers, waveguide couplers, and detectors for increased circuit functionality [10]. In addition, since SOAs provide amplification, they allow high fan–out and high cascadability, requirements for large photonic circuits and multi-component lightwave systems in general [6].

For most applications, a disadvantage of resonant-type bistable switching is that it occurs over a limited spectral range [1], [11]. (An exception is wavelength-division demultiplexing, where the narrow spectral response is used to select the desired signal [7].) One way to alter the bistable behavior of a DFB device is to change the uniformity of the built-in grating, as was shown for passive [12]–[15] and active [16], [17] devices. In this paper, we study the effects of spatial chirp of the built-in grating on the spectral range and threshold power of switching in DFB SOAs. Our goal is to increase the spectral range of low-power switching, thereby making DFB SOAs more suitable for lightwave technologies.

#6998 - $15.00 US
Received October 01, 1998; Revised October 19, 1998

This paper is organized as follows. In Section 2, we review our computational model, and use it in Section 3 to examine switching in a uniform-grating device. In Section 4, spatial chirp is introduced and its effects on the full spectral range of switching are investigated. By considering switching at both sides of the stop band, we identify a case which exhibits a large increase in the spectral range of low-power switching. Issues arising for switching in devices with large amounts of spatial chirp are discussed in Section 5.

2. Numerical Model

We study bistability in DFB SOAs with the following model. Since an optical field with a wavelength in the vicinity of the Bragg wavelength interacts with the grating, its z dependence is conveniently expressed as the sum of two counterpropagating modes:

$$\vec{E}(x,y,z,t) = \mathrm{Re}\{\vec{\epsilon}F(x,y)[A(z)\exp(i\beta_B z) + B(z)\exp(-i\beta_B z)]\exp(-i\omega t)\}, \quad (1)$$

where A and B are the slowly varying field envelopes, $\beta_B = \pi/\Lambda$ is the Bragg wavenumber associated with the grating period Λ, Re stands for the real part, $\vec{\epsilon}$ is the unit vector along the direction of polarization, $F(x,y)$ represents the transverse variation of the fundamental mode supported by the waveguide, and ω is the optical frequency.

For continuous-wave signals and pulses much longer than the carrier lifetime, the field distribution inside the DFB SOA can be calculated via the following coupled-mode equations:

$$\frac{dA}{dz} = \left[i\delta + \frac{g_0}{2}\frac{(1-i\alpha)}{1+\bar{P}} - \frac{\alpha_{int}}{2}\right]A + i\kappa B, \quad (2)$$

$$-\frac{dB}{dz} = \left[i\delta + \frac{g_0}{2}\frac{(1-i\alpha)}{1+\bar{P}} - \frac{\alpha_{int}}{2}\right]B + i\kappa A. \quad (3)$$

Here, κ is the coupling coefficient, α_{int} accounts for internal losses, and g_0 is the small-signal gain coefficient. The detuning parameter δ is given by

$$\delta = \beta_0 - \beta_B = \frac{2\pi n_0}{\lambda_0} - \frac{\pi}{\Lambda}, \quad (4)$$

where β_0 and n_0 are the carrier-density-*independent* parts of the signal wavenumber and the average modal refractive index, respectively. The detuning δ is related to the free-space signal wavelength λ_0 such that, for constant n_0 and Λ, smaller values of detuning correspond to longer signal wavelengths.

The carrier-density-dependent contribution to the signal wavenumber is represented by $\alpha g_0/[2(1+\bar{P})]$ in the coupled-mode equations. The linewidth enhancement factor α represents coupling between the refractive index and optical gain that occurs in active semiconductor media, and is the source of nonlinearity responsible for the bistability in this study. Unlike a Kerr nonlinearity, the dependence on the optical field is of the form $(1+\bar{P})^{-1}$. The quantity $\bar{P} = P/P_{sat}$ is the optical power normalized to the saturation power. In terms of the field envelopes, the normalized power is given by

$$\bar{P} = \frac{|E|^2\sigma}{P_{sat}} \approx [|A(z)|^2 + |B(z)|^2]\frac{\Gamma\sigma}{P_{sat}}, \quad (5)$$

where σ is the cross section and Γ is the confinement factor of the optical mode.

We solve Eqs. (2) and (3) via a transfer-matrix method in which the amplifier is represented by an array of transfer matrices [17]. Each matrix corresponds to an approximately uniform section of the DFB amplifier, and is calculated from the analytic solution for a linearized form of Eqs. (2) and (3). Using the boundary condition at the output facet B(L) = 0 and neglecting facet reflections, the internal-power distribution along the amplifier is calculated

#6998 - $15.00 US Received October 01, 1998; Revised October 19, 1998

with this transfer-matrix array, and is used to saturate the gain in each section. Values for the internal power and saturated gain along the device are calculated iteratively until convergence. We refer the readers to Ref. [17] for a more thorough discussion of these equations and method of solution.

3. Uniform Gratings

An example of the bistable transmission through a uniform-grating DFB SOA is shown in Fig. 2(a), for $\kappa L = 3$, $\alpha_{int} = 0$, $g_0 L = 1.198$, $\delta L = 6.785$, $\alpha = 5$, and P_{sat} = 10 mW. These typical parameter values were used in Fig. 1(b) and are used throughout this paper except for changes in the normalized detuning δL and small-signal gain $g_0 L$. As seen in Fig. 2(a), switching from the lower stable branch to the upper stable branch (solid lines) occurs near 24 μW, and the switched signal experiences an on-state gain of about 15 dB.

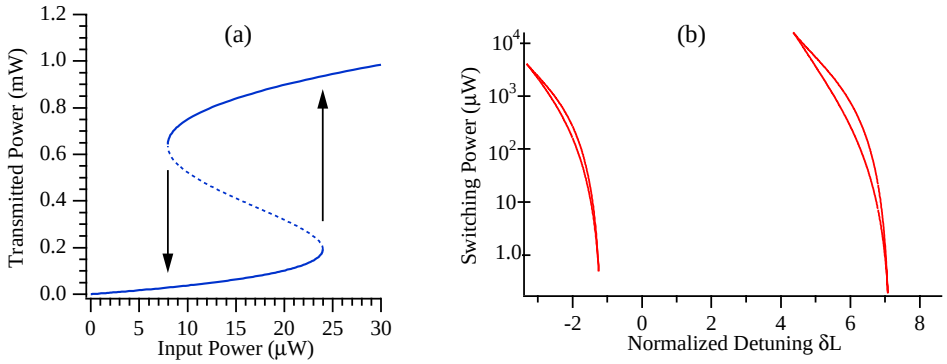

Figure 2. (a) Bistable transmission for $\delta L = 6.785$ and $P_{sat} = 10$ mW. Switching occurs between the stable branches, as indicated. (b) Upward- and downward- switching input powers plotted over the entire spectral range of switching.

The hysteresis in Fig. 2(a) is for a specific value of the detuning ($\delta L = 6.785$). To illustrate the *entire* spectral range of switching, the input powers required for upward and downward switching are given in Fig. 2(b) as a function of δL. The low-power onset of switching for each of the two spectral regions shown in Fig. 2(b) occurs at a value of δL near a small-signal transmittivity peak [see Fig. 1(b)]. The switching powers increase from the onset values as the signal is tuned to longer wavelengths (i.e. smaller values of δL). These two spectral regions, referred to simply as the long- and short-wavelength sides of the stop band, exhibit a spectral range of about 2 and 2.7 δL, respectively. This corresponds to a spectral range of 0.73 nm (91 GHz) and 0.98 nm (123 GHz), respectively, for a 300-μm-long device operating near 1.55 μm.

Switching powers in Fig. 2(b) range from 1 μW to 10 mW. A more important spectral range is that for which the upward-switching power remains below a level that is practical for optical communication systems. We choose this power level to be 0.1 mW. The spectral range of switching below 0.1 mW is only 0.51 δL, or about 0.19 nm (23 GHz), for switching at both sides of the stop band. To increase this spectral range, we introduce spatial chirp into the built-in grating.

4. Chirped Gratings

A DFB SOA with a linearly chirped grating is depicted schematically in Fig. 3. The P–direction (N–direction) is defined to be the direction for which an incident optical signal sees an increase (decrease) in the spatial frequency of the grating. The direction is specified in calculations by

#6998 - $15.00 US
Received October 01, 1998; Revised October 19, 1998

the sign of the chirp parameter C, introduced by using

$$\beta_B(z) = \bar{\beta}_B + \frac{C}{L^2}\left(z - \frac{L}{2}\right), \tag{6}$$

where $\bar{\beta}_B$ is the average Bragg wavenumber. A positive (negative) value of C corresponds to the P–direction (N–direction), and the magnitude of C represents the total change in $\beta_B(z)L$ along the device. For small amounts of spatial chirp, the coupled-mode equations (2) and (3) remain unchanged except that the detuning parameter $\delta = \beta_0 - \beta_B$ now becomes z dependent. For example, a value of $|C| = 10$ corresponds to a total variation in β_B of about 0.24% for a 300-μm-long device.

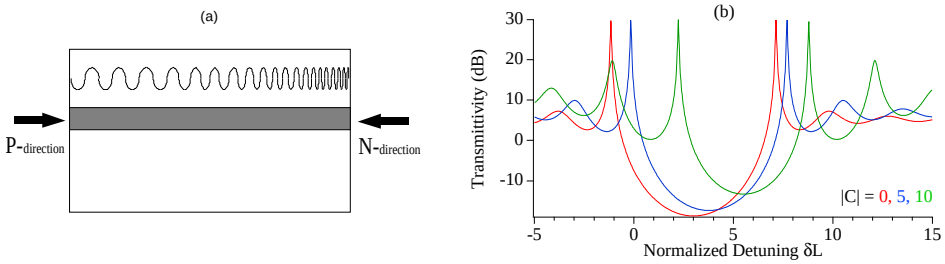

Figure 3. (a) Schematic illustration of a DFB SOA with a linearly chirped grating, indicating the P–direction ($C > 0$) and N–direction ($C < 0$). (b) Small-signal transmittivity spectra for three chirped gratings for the case of 30-dB amplification.

Since the Bragg wavenumber varies along the length of a chirped-grating device, the feedback within the structure is significantly altered. An increase in the amount of linear chirp weakens the feedback such that the lasing threshold increases [18]. Likewise, the amount of gain required to maintain transmission resonances that provide 30 dB of small-signal amplification also increases. For $|C|$ = 0, 5, 10, the required values of g_0L are 1.198, 1.508, and 2.206, respectively, and are used in Fig. 3(b) to plot the transmittivity spectra. The shift of the stop band to higher values of detuning δL accompanying an increase in gain results from defining δL to be independent of the carrier density [see Eq. (4)]. We drive all chirped amplifiers to provide 30-dB small-signal amplification when comparing switching characteristics.

The effect of spatial chirp on the entire spectral range for switching at either side of the stop band is shown in Fig. 4. The switching powers are given in terms of the normalized power $\bar{P}$ (left axis) and for a specific value of $P_{sat} = 10$ mW (right axis). Linear spatial chirp tends to increase the spectral range of bistable switching for signals incident in either the P-direction or N-direction. The largest percent increase in the spectral range occurs at the long-wavelength side of the stop band for signals traveling in the N-direction. For $C = -10$, a 92% increase results in a spectral width of $\delta L = 3.97$. The broadest total spectral range in Fig. 4, however, is exhibited by switching at the short-wavelength side of the stop band for $C = -10$, and is 5.1 δL, or 1.86 nm (232 GHz). The blue shift of the low-power onset of switching follows the shift of the transmission peaks with increasing gain, as shown in Fig. 3(b).

Although signals incident on the short-wavelength side of the stop band with $C = -10$ exhibit the broadest total spectral range, switching powers tend to *increase* with spatial chirp. This is consistent with the effect of spatial chirp in passive Kerr-nonlinear devices for switching at the center of the stop band [12]. Most notably, the low-power onset of bistability increases with spatial chirp. Considering switching powers less than 0.1 mW, the spectral range is only 0.36 δL, or 0.13 nm (16 GHz). Using $P_{sat} = 10$ mW, the 0.1-mW power level corresponds to 0.1 $\bar{P}$ and is indicated by the dotted lines in Fig. 4.

#6998 - $15.00 US
Received October 01, 1998; Revised October 19, 1998

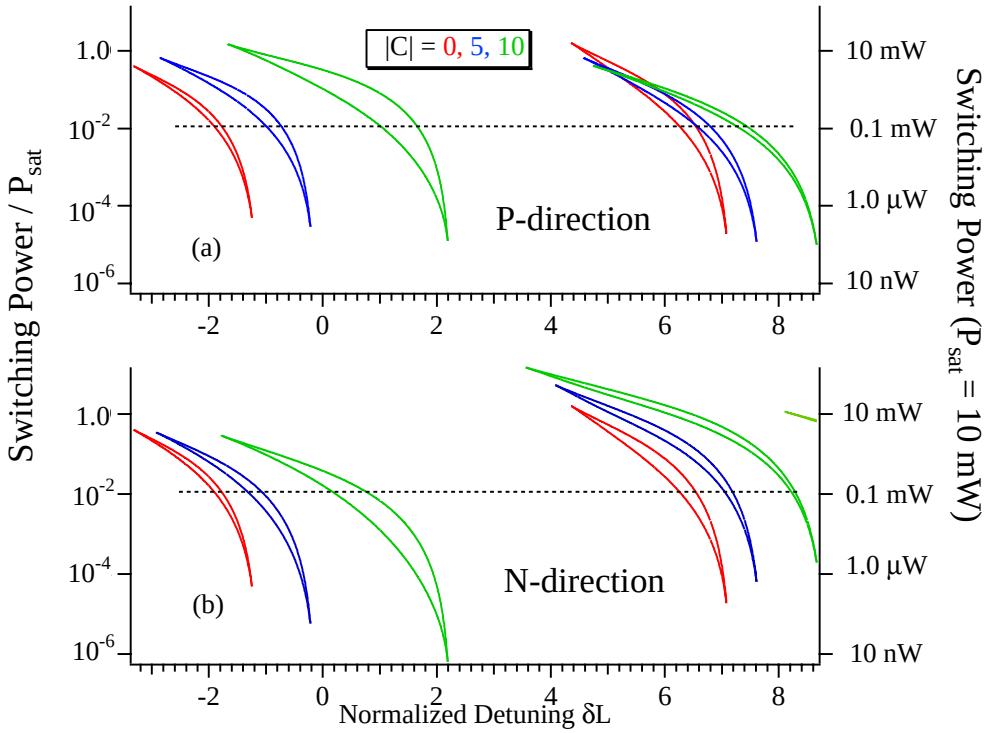

Figure 4. Spectral range of bistable switching for optical signals incident in the (a) P–direction and (b) N–direction of a chirped-grating DFB SOA. The long-wavelength side of (b) for $C = -10$ exhibits the lowest switching power and the broadest spectral range of low-power switching.

For optical signals on the blue-side of the stop band and traveling in the *P*–direction, switching powers tend to *decrease* with spatial chirp. This is also consistent with studies in passive Kerr-nonlinear devices for switching at the center of the stop band. In particular, the onset of switching gradually decreases with increasing spatial chirp and is 0.1 μW for $C = 10$. As a result, the spectral range of low-power switching is twice as wide as that for an unchirped grating.

For switching at the *long*-wavelength side of the stop band, optical signals incident in both directions see a decrease in the onset of switching with an increase in spatial chirp. Most notably, for $C = -10$, the switching power at the onset of bistability drops below the very low level of 10 nW — two orders of magnitude lower than its value for $C = 0$. Consequently, this case exhibits the widest spectral range of low-power switching; the spectral range is 1.37 δL (0.5 nm, or 62 GHz), an increase of 2.7 times from the unchirped case.

5. Large Chirp

For large amounts of spatial chirp, resonances away from the stop band tend to become stronger. This is apparent in Fig. 3(b); for $|C| = 10$, the outer resonances provide about 20-dB amplification. One consequence is that strong outer resonances can give rise to bistable switching in the *same* spectral region as a neighboring resonance. This behavior is seen in Fig. 4(b) for the case $C = -10$ in the spectral region from 8.1 to 8.67 δL. Here, optical signals experience two hystereses in their transmitted power, as shown in Fig. 5(a) for δL = 8.4. This behavior has interesting applications as a two-level optical memory, or optical switch. We expect that a prudent choice of device parameters (e.g., spatial chirp C, coupling coefficient κ) will bring the switching powers of both bistable regions closer, for practical device operation.

#6998 - $15.00 US
Received October 01, 1998; Revised October 19, 1998

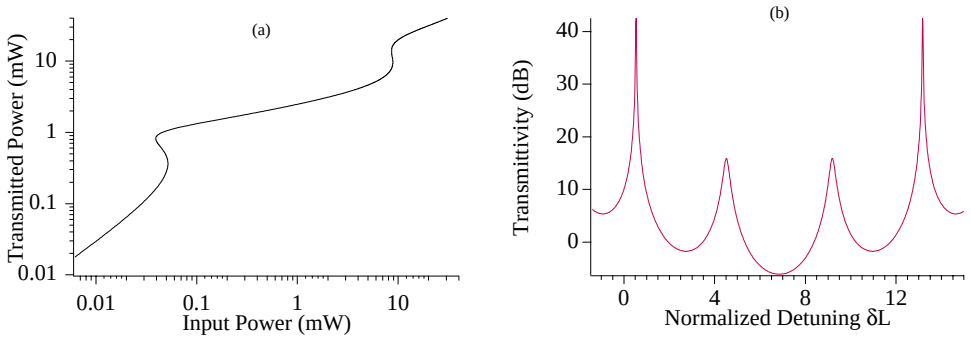

Figure 5. (a) Double bistability. (b) Transmission through a DFB SOA with $|C| = 15$ driven at 98% of its lasing threshold.

For large amounts of linear spatial chirp, resonances away from the stop band can become strong enough that they exhibit the lowest lasing threshold [18]. This behavior is shown in Fig. 5(b) for $|C| = 15$ for a value of $g_0 L$ (= 2.74) equivalent to 98% of the (unsaturated) lasing threshold. Under such conditions, the inner resonances are unable to provide 30-dB amplification. Therefore, the outer resonances should be used for high-gain optical switching. ¿From a computational perspective, *any* value of $g_0 L$ can be used in calculations, but only one that lies below lasing threshold is physically important, since the device is not used as a laser. Thus, care must be taken during the study and design of chirped-grating DFB SOAs to track the lasing threshold, an issue that does not exist for passive Kerr-nonlinear devices.

6. Conclusion

We found that introducing a linear spatial chirp of 0.24% into the built-in grating reduces the switching power at the onset of bistability by two orders of magnitude. For typical device parameters, this corresponds to 10-nW switching. Moreover, the spectral range of switching below 0.1 mW is increased 2.7 times to a range of 1.37 δL. For a 300-μm-long device operating near 1.55 μm, this spectral range is 0.5 nm (62 GHz), as opposed to 0.19 nm (23 GHz) for an unchirped device. These improvements occur on the long-wavelength side of the stop band for optical signals propagating in the N–direction.

Since dense WDM communication systems have a channel spacing of 1 nm or less, a spectral range of 0.5 nm provides enough wavelength flexibility for chirped-grating DFB SOAs to add or drop individual channels. Also, chirped-grating DFB SOAs have enough bandwidth that they can be used to switch 10 Gb/s signals, provided that the device has a response time of about 100 ps. For uniform-grating DFB SOAs, the carrier lifetime is only about 1 ns. Fortunately, the carrier lifetime is likely to reduce for linearly chirped gratings since the SOA can be operated at higher carrier densities without reaching lasing threshold. Since a doubling of the carrier density can reduce the carrier lifetime by a factor of eight when the Auger recombination dominates [1], we expect that lifetimes $\sim$ 100 ps are feasible, thus making chirped-grating DFB SOAs applicable to 10 Gb/s optical communication systems.

Acknowledgments

The authors would like to thank the reviewers for their insightful comments. This research was supported by the U.S. Department of Education and by the National Science Foundation.

#6998 - $15.00 US Received October 01, 1998; Revised October 19, 1998